Chapter 9
Niue

9.1 Climate Summary

9.1.1 Current Climate

- Annual and half-year mean temperatures have warmed at Alofi-Hanan Airport since 1940.
- The frequency of Warm Days and Warm Nights has significantly increased while Cool Days have decreased at Alofi-Hanan Airport.
- Annual and half-year rainfall trends show little change at Alofi-Hanan Airport since 1905. There has also been little change in extreme rainfall since 1915.
- Tropical cyclones affect Niue mainly between November and April. An average of 10 cyclones per decade developed within or crossed the Niue Exclusive Economic Zone (EEZ) between the 1969/70 and 2010/11 seasons. Six of the 24 tropical cyclones (25%) between the 1981/82 and 2010/11 seasons became severe events (Category 3 or stronger) in the Niue EEZ. Available data are not suitable for assessing long-term trends.

- Wind-waves at Niue have a nearly constant height period and direction throughout the year, with a slight seasonal increase in wave height and period with southern trade winds. Waves are characterised by trade winds seasonally and the El Niño–Southern Oscillation (ENSO) and Southern Annular Mode (SAM) interannually. Available data are not suitable for assessing long-term trends (see Section 1.3).

9.1.2 Climate Projections

For the period to 2100, the latest global climate model (GCM) projections and climate science findings indicate:

- El Niño and La Niña events will continue to occur in the future (*very high confidence*), but there is little consensus on whether these events will change in intensity or frequency;
- Annual mean temperatures and extremely high daily temperatures will continue to rise (*very high confidence*);

- Mean annual rainfall could increase or decrease with the model average indicating little change (*low confidence* in this model average), with more extreme rain events (*high confidence*);
- The proportion of time in drought is projected to increase or decrease in line with average rainfall (*low confidence*);
- Ocean acidification is expected to continue (*very high confidence*);
- The risk of coral bleaching will increase in the future (*very high confidence);*
- Sea level will continue to rise (*very high confidence*); and
- Wave heights may decrease in December–March (*low confidence)*, with no significant changes projected in June–September waves (*low confidence)*.

9.2 Data Availability

There are currently two operational meteorological observation stations on Niue. The primary station, where multiple observations are conducted on a daily basis, is located at Hanan Airport, south of Alofi on the western side of the island. A single daily observation rainfall station is located at Liku on the eastern side of the island. Observations began at Liku in 1990. The complete historical record for Hanan Airport, Alofi and Kaimiti has been used to create a Hanan Airport composite. Observations were taken close to the Alofi wharf from 1905 to 1971 and adjacent to the current Alofi Police Station from 1977 to 1996. Between 1971 and 1976 observations were taken at Kaimiti, 2.4 km south of Alofi. Hanan Airport monthly rainfall from 1905 (daily values from 1915) and air temperature from 1940 have been used in this report. The Hanan Airport composite record is homogeneous. Additional information on historical climate trends in the Niue region can be found in the Pacific Climate Change Data Portal www.bom.gov.au/climate/pccsp/.

Wind-wave data from buoys are particularly sparse in the Pacific region, with very short records. Model and reanalysis data are therefore required to detail the wind-wave climate of the region. Reanalysis surface wind data have been used to drive a wave model over the period 1979–2009 to generate a hindcast of the historical wind-wave climate.

9.3 Seasonal Cycles

Information on temperature and rainfall seasonal cycles can be found in Australian Bureau of Meteorology and CSIRO (2011).

9.3.1 Wind-driven Waves

The wind-wave climate of Niue is strongly characterised by the Southern Hemisphere trade winds. On the west coast, where easterly waves may be blocked by the island, waves are directed from the south year round, with more directional variability during December–March. Swell is observed from the south to south-west year round due to Southern Ocean storms. Wave heights and period are slightly smaller in December–March, when mean height is around 1.8 m and mean period around 9.9 s, than June–September, when mean height is around 2.1 m and period around 10.3 s (Table 9.1, Figure 9.1). Waves larger than 3.6 m (99th percentile) occur year round, usually from the south and south-west, due to Southern Ocean swell waves. Large northerly and westerly waves, associated with cyclones, are seen in December–March. The height of a 1-in-50 year wave event on the west coast of Niue is calculated to be 10.2 m.

No suitable dataset is available to assess long-term historical trends in the Niue wave climate. However, interannual variability may be assessed in the hindcast record. The wind-wave climate displays strong interannual variability at Niue, varying strongly with ENSO in December–March and SAM in both December–March and June–September. During El Niño years, southerly wave power is greater than during La Niña years in December–March due to movement of the South Pacific Convergence Zone (SPCZ) away from Niue. Wave power is similar during June–September in both phases of ENSO, slightly weaker during La Niña, with waves directed more from the east in these months in La Niña years associated with increased trade winds. When the Southern Annular Mode (SAM) index is negative there is a strong rotation of waves toward the south-west due to enhanced extra-tropical storms in the Southern Ocean, with a 50% increase in wave power in December–March and a slight reduction in June–September.

Table 9.1: Mean wave height, period and direction from which the waves are travelling near Niue in December–March and June–September. Observation (hindcast) and climate model simulation mean values are given with the 5–95th percentile range (in brackets). Historical model simulation values are given for comparison with projections (see Section 9.5.6 – Wind-driven waves, and Table 9.7). A compass relating number of degrees to cardinal points (direction) is shown.

		Hindcast Reference Data (1979–2009)	Climate Model Simulations (1986–2005)
Wave Height (metres)	December–March	1.8 (1.2–2.8)	2.0 (1.6–2.3)
	June–September	2.1 (1.4–3.1)	2.2 (1.7–2.6)
Wave Period (seconds)	December–March	9.9 (7.9–12.2)	8.9 (7.9–10.2)
	June–September	10.3 (8.0–12.9)	8.9 (7.7–9.8)
Wave Direction (degrees clockwise from North)	December–March	180 (40–320)	90 (60–130)
	June–September	180 (140–220)	150 (130–170)
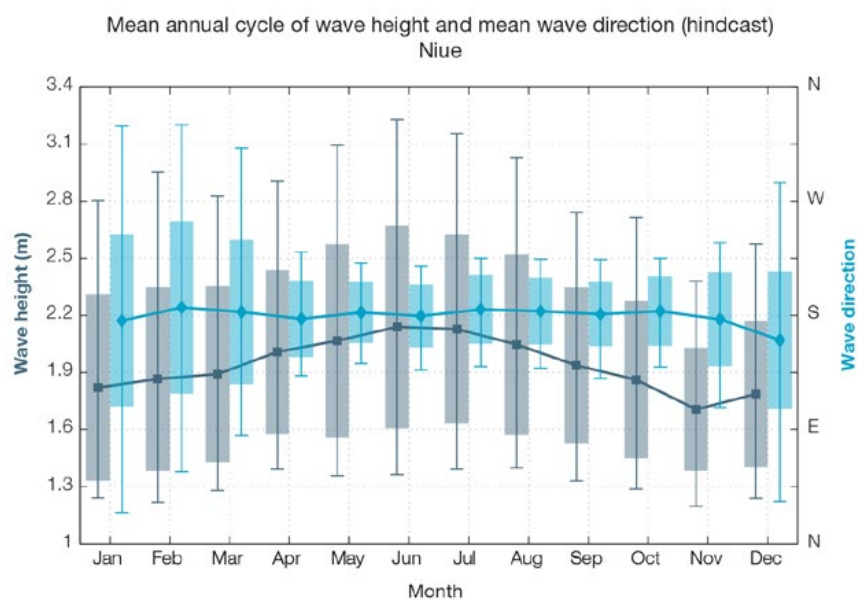
Figure 9.1: Mean annual cycle of wave height (grey) and mean wave direction (blue) at Niue in hindcast data (1979–2009). To give an indication of interannual variability of the monthly means of the hindcast data, shaded boxes show 1 standard deviation around the monthly means, and error bars show the 5–95% range. The direction from which the waves are travelling is shown (not the direction towards which they are travelling).

9.4 Observed Trends

9.4.1 Air Temperature

Annual and Half-year Mean Air Temperature

Warming trends are evident in November–April maximum and minimum temperatures at Alofi-Hanan Airport for the period 1940–2011 (Figure 9.2 and Table 9.2). The strongest trend is in minimum temperatures for November to April. All the temperature trends are consistent with regional and global warming trends.

Table 9.2: Annual and half-year trends in air temperature (Tmax, Tmin, Tmean) and rainfall at Alofi-Hanan Airport. The 95% confidence intervals are shown in brackets. Values for trends significant at the 5% level are shown in **boldface**.

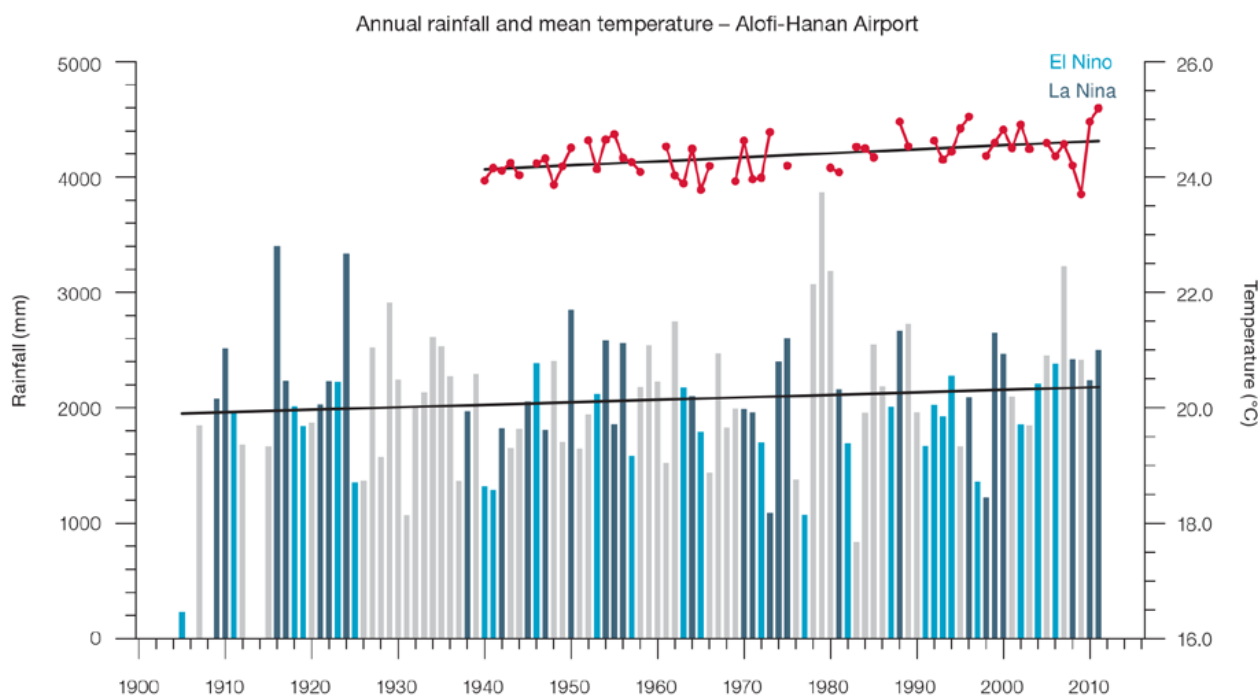| Alofi-Hanan Airport	Tmax (°C/10yrs)	Airport Tmin (°C/10yrs) 1940–2011	Tmean (°C/10yrs)	Total Rain (mm/10yrs) 1905–2011
Annual	-	-	-	+2.20 (-25.6, +29.7)
Nov–Apr	**+0.06** (0.00, +0.10)	**+0.12** (+0.05, +0.19)	-	+12.20 (-9.8, +29.6)
May–Oct	+0.02 (-0.01, +0.08)	+0.07 (-0.01, +0.13)	+0.05 (-0.01, +0.1)	0.00 (-0.30, +0.30)

Figure 9.2: Observed time series of annual average values of mean air temperature (red dots and line) and total rainfall (bars) at Alofi-Hanan Airport. Light blue, dark blue and grey bars denote El Niño, La Niña and neutral years respectively. Solid black trend lines indicate a least squares fit.

Extreme Daily Air Temperature

Extreme daily temperatures have warmed at Alofi-Hanan Airport (Figure 9.3 and Table 9.3). The number of Warm Days and Warm Nights have significantly increased while Cool Days have decreased. These trends are statistically significant at the 5% level and consistent with regional and global warming trends.

9.4.2 Rainfall

Annual and Half-year Total Rainfall

Notable interannual variability associated with the ENSO is evident in the observed rainfall record for Alofi-Hanan Airport since 1905 (Figure 9.2). Trends in annual and half-year rainfall shown in Table 9.2 and Figure 9.2 are not statistically significant at the 5% level. In other words, annual and half-year rainfall trends show little change at Alofi-Hanan Airport.

Daily Rainfall

Daily rainfall trends for Alofi-Hanan Airport are presented in Table 9.3. Due to large year-to-year variability, there are no significant trends in the daily rainfall indices. Figure 9.4 shows insignificant trends in annual Max 1-day rainfall and Rain Days ≥ 1 mm (days with rainfall).

Table 9.3: Annual trends in air temperature and rainfall extremes at Alofi-Hanan Airport. The 95% confidence intervals are shown in parentheses. Values for trends significant at the 5% level are shown in boldface.

	Alofi-Hanan Airport
TEMPERATURE	**(1940–2011)**
Warm Days (days/decade)	**+3.90** (+0.46, +7.20)
Warm Nights (days/decade)	**+3.97** (+1.22, +7.12)
Cool Days (days/decade)	**-5.77** (-7.85, -3.95)
Cool Nights (days/decade)	-1.80 (-4.81, +1.28)
RAINFALL	**(1915–2011)**
Rain Days ≥ 1 mm (days/decade)	+1.48 (-0.35, +3.22)
Very Wet day rainfall (mm/decade)	-7.93 (-36.64, +22.25)
Consecutive Dry Days (days/decade)	0.00 (-0.34, +0.32)
Max 1-day rainfall (mm/decade)	-1.17 (-4.66, +2.26)

Warm Days: Number of days with maximum temperature greater than the 90th percentile for the base period 1971–2000
Warm Nights: Number of days with minimum temperature greater than the 90th percentile for the base period 1971–2000
Cool Days: Number of days with maximum temperature less than the 10th percentile for the base period 1971–2000
Cool Nights: Number of days with minimum temperature less than the 10th percentile for the base period 1971–2000
Rain Days ≥ 1 mm: Annual count of days where rainfall is greater or equal to 1 mm (0.039 inches)
Very Wet Day rainfall: Amount of rain in a year where daily rainfall is greater than the 95th percentile for the reference period 1971–2000
Consecutive Dry Days: Maximum number of consecutive days in a year with rainfall less than 1mm (0.039 inches)
Max 1-day rainfall: Annual maximum 1-day rainfall
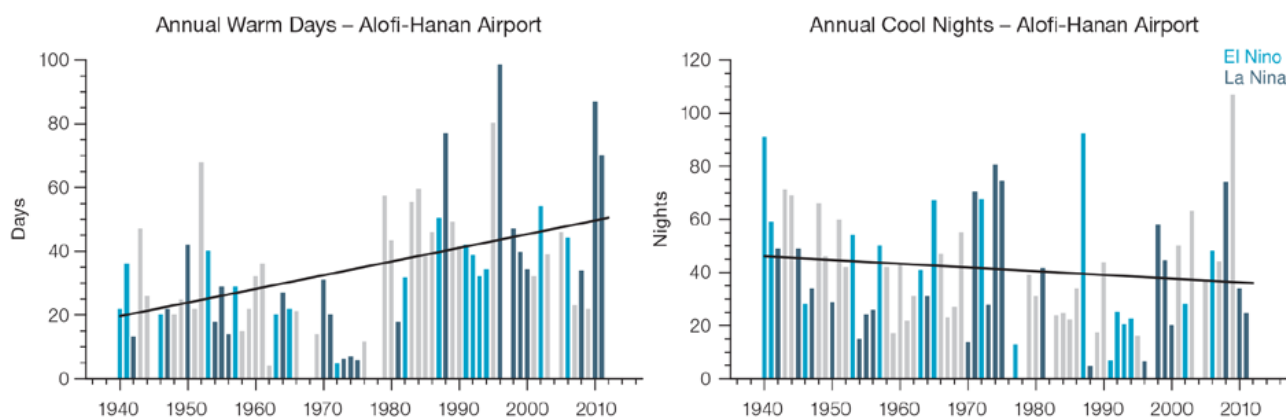
Figure 9.3: Observed time series of annual total number of Warm Days (left) and Cool Nights (right) at Alofi-Hanan Airport. Solid black trend lines indicate a least squares fit.
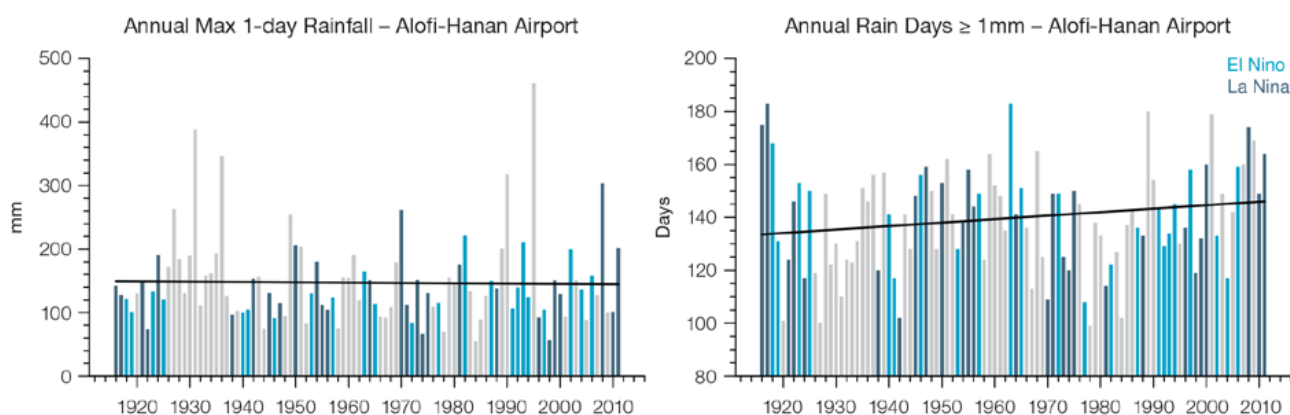
Figure 9.4: Observed time series of annual Max 1-day rainfall (left) and Rain Days ≥ 1 mm at Alofi-Hanan Airport (right). Solid black trend lines indicate a least squares fit.
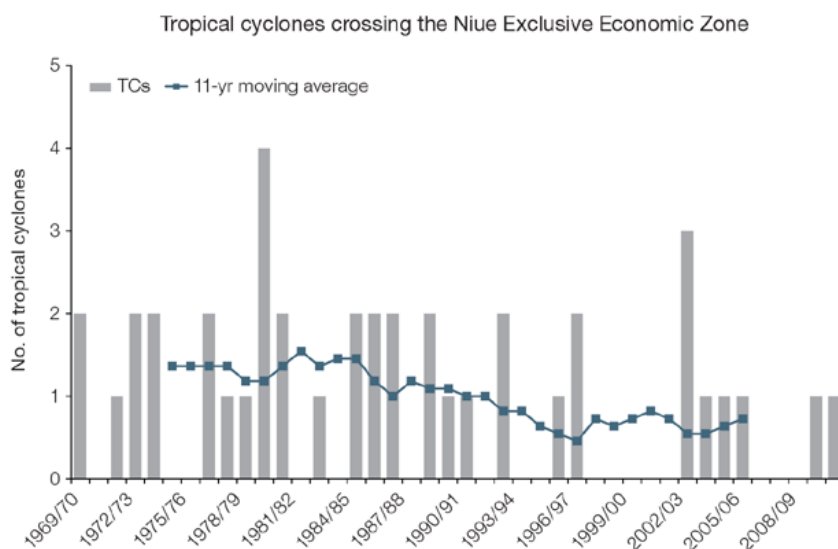
9.4.3 Tropical Cyclones

Tropical cyclones affect Niue between November and April. Occurrences outside this period are rare. The tropical cyclone archive for the Southern Hemisphere indicates that between the 1969/70 and 2010/11 seasons, 41 tropical cyclones developed within or crossed the Niue EEZ. This represents an average of 10 cyclones per decade. Refer to Chapter 1, Section 1.4.2 (Tropical Cyclones) for an explanation of the difference in the number of tropical cyclones occurring in Niue in this report (Australian Bureau of Meteorology and CSIRO, 2014) compared to Australian Bureau of Meteorology and CSIRO (2011).

The interannual variability in the number of tropical cyclones in the Niue EEZ is large ranging from zero in some seasons to four in the 1979/80 season (Figure 9.5). The differences between tropical cyclone average occurrence in El Niño, La Niña and neutral years are not statistically significant. Six of the 24 tropical cyclones (25%) between the 1981/82 and 2010/11 seasons became severe events (Category 3 or stronger) in the Niue EEZ.

Long term trends in frequency and intensity have not been presented as country scale assessment is not recommended. Some tropical cyclone tracks analysed in this subsection include the tropical depression stage (sustained winds less than or equal to 34 knots) before and/or after tropical cyclone formation.

Additional information on historical tropical cyclones in the Niue region can be found at www.bom.gov.au/cyclone/history/tracks/index.shtml

Figure 9.5: Time series of the observed number of tropical cyclones developing within and crossing the Niue EEZ per season. The 11-year moving average is in blue.

9.5 Climate Projections

The performance of the available Coupled Model Intercomparison Project (Phase 5) (CMIP5) climate models over the Pacific has been rigorously assessed (Brown et al., 2013a, b; Grose et al., 2014; Widlansky et al., 2013). The simulation of the key processes and features for the Niue region is similar to the previous generation of CMIP3 models, with all the same strengths and many of the same weaknesses. The best-performing CMIP5 models used here have lower biases (differences between the simulated and observed climate data) than the best CMIP3 models, and there are fewer poorly-performing models. For Niue, the most important model bias is that the rainfall maximum of the SPCZ is too zonally (east-west) oriented and does not extend in a diagonal band to the southeast of

Niue. This lowers confidence in the model projections. Out of 27 models assessed, three models were rejected for use in these projections due to biases in the mean climate and in the simulation of the SPCZ. Climate projections have been derived from up to 24 new global climate models (GCMs) in the CMIP5 database (the exact number is different for each scenario, Appendix A), compared with up to 18 models in the CMIP3 database reported in Australian Bureau of Meteorology and CSIRO (2011).

It is important to realise that the models used give different projections under the same scenario. This means there is not a single projected future for Niue, but rather a range of possible futures for each emission scenario. This range is described below.

9.5.1 Temperature

Further warming is expected over Niue (Figure 9.6, Table 9.6). Under all RCPs, the warming is up to 1.1°C by 2030, relative to 1995, but after 2030 there is a growing difference in warming between each RCP. For example, in Niue by 2090, a warming of 1.7 to 4.2°C is projected for RCP8.5 (very high emissions) while a warming of 0.2 to 1.1°C is projected for RCP2.6 (very low emissions). This range is broader than that presented in Australian Bureau of Meteorology and CSIRO (2011) because a wider range of emissions scenarios is considered. While relatively warm and cool years and decades will still occur due to natural variability, there is projected to be more warm years and decades on average in a warmer climate.
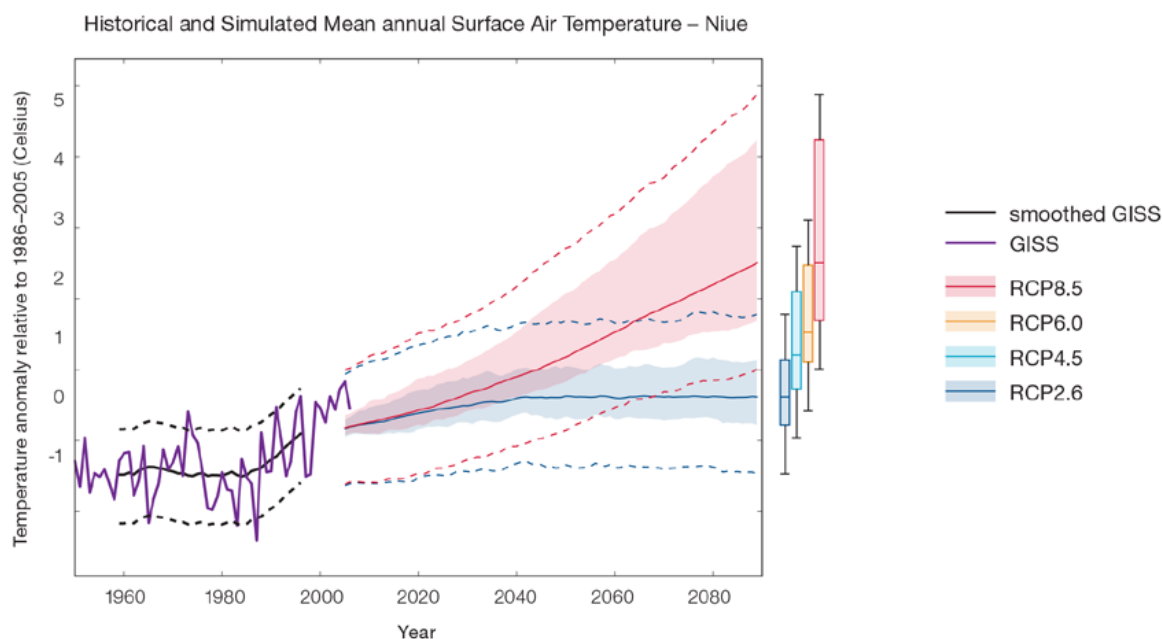
Figure 9.6: Historical and simulated surface air temperature time series for the region surrounding Niue. The graph shows the anomaly (from the base period 1986–2005) in surface air temperature from observations (the GISS dataset, in purple), and for the CMIP5 models under the very high (RCP8.5, in red) and very low (RCP2.6, in blue) emissions scenarios. The solid red and blue lines show the smoothed (20-year running average) multi-model mean anomaly in surface air temperature, while shading represents the spread of model values (5–95th percentile). The dashed lines show the 5–95th percentile of the observed interannual variability for the observed period (in black) and added to the projections as a visual guide (in red and blue). This indicates that future surface air temperature could be above or below the projected long-term averages due to interannual variability. The ranges of projections for a 20-year period centred on 2090 are shown by the bars on the right for RCP8.5, 6.0, 4.5 and 2.6.

There is *very high confidence* that temperatures will rise because:

- It is known from theory and observations that an increase in greenhouse gases will lead to a warming of the atmosphere; and

- Climate models agree that the long-term average temperature will rise.

There is *medium confidence* in the model average temperature change shown in Table 9.6 because:

- The new models do not simulate the temperature change of the recent past in Niue as well as in other places; and

- There is a bias in the simulation of the current SPCZ near Niue, and uncertainty in the projection of the SPCZ, which not only affects the current bias and uncertainty in projections of rainfall but also temperature.

9.5.2 Rainfall

The CMIP5 models show a range of projected annual mean rainfall change from an increase to a decrease, and the model average is for a slight increase for the high emission scenario by the end of the century. The range is greater in the highest emissions scenarios (Figure 9.7, Table 9.6). Similar to the CMIP3 results, there is greater model agreement for a slight increase in November–April rainfall (more than two thirds of models), and little change in May–October rainfall. There was greater confidence in the projected change in November–April rainfall in the previous report, however new research has raised more uncertainty about the future of the SPCZ (see Box in Chapter 1 for more details). Mean rainfall increased in Niue between 1979 and 2006 (Figure 9.7),

but the models do not project this will continue at the same rate into the future. This indicates that the recent increase may be caused by natural variability and not caused by global warming. It is also possible that the models do not simulate a key process driving the recent change. However, the recent change is not particularly large (<10%) and the observed record shown is not particularly long (28 years), so it is difficult to determine the significance of this difference, and its cause. The year-to-year rainfall variability over Niue is generally larger than the projected change, except for the models with the largest projected change in the highest emission scenario by 2090. The effect of climate change on average rainfall may not be obvious in the short or medium term due to natural variability.
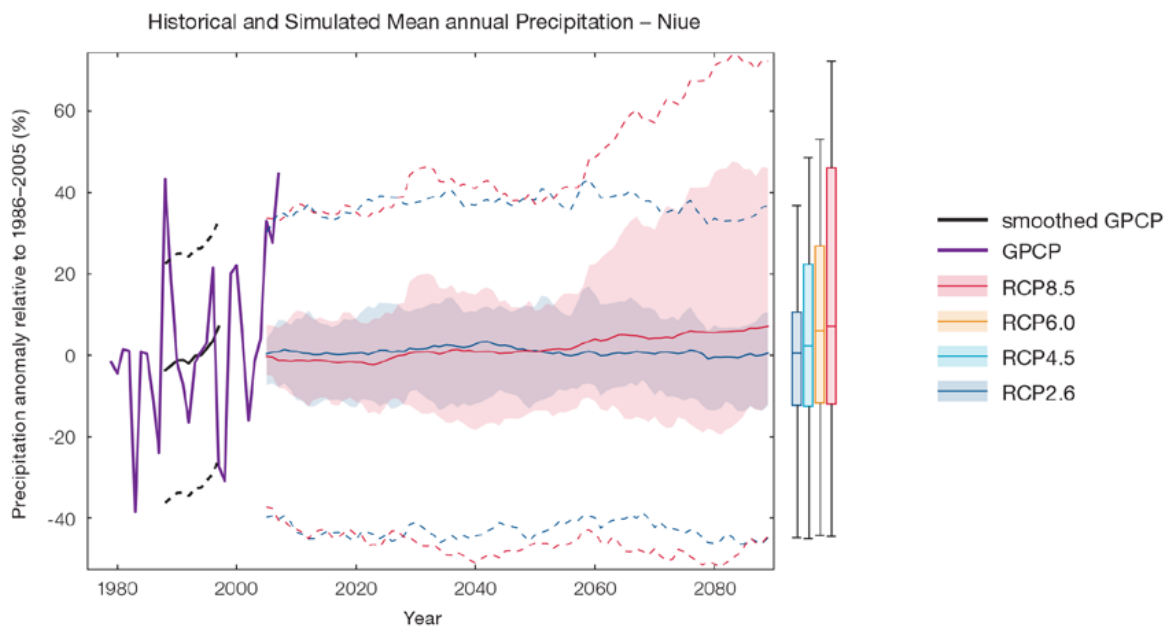
Figure 9.7: Historical and simulated annual average rainfall time series for the region Niue. The graph shows the anomaly (from the base period 1986–2005) in rainfall from observations (the GPCP dataset, in purple), and for the CMIP5 models under the very high (RCP8.5, in red) and very low (RCP2.6, in blue) emissions scenarios. The solid red and blue lines show the smoothed (20-year running average) multi-model mean anomaly in rainfall, while shading represents the spread of model values (5–95th percentile). The dashed lines show the 5–95th percentile of the observed interannual variability for the observed period (in black) and added to the projections as a visual guide (in red and blue). This indicates that future rainfall could be above or below the projected long-term averages due to interannual variability. The ranges of projections for a 20-year period centred on 2090 are shown by the bars on the right for RCP8.5, 6.0, 4.5 and 2.6.

The model mean shows an increase in rainfall, but not all models agree. This lowers the confidence that we can determine the most likely direction of change in annual rainfall, and makes the amount difficult to determine. The 5–95th percentile range of projected values from CMIP5 climate models is large, e.g. for RCP8.5 (very high emissions) the range is -12 to +18% by 2030 and -12 to +46% by 2090.

There is *low confidence* in the model average result of slight increase in annual rainfall for Niue because:

- This average finding of no change is the average of a model spread from a projected rainfall increase to a rainfall decrease, and also many models project little change; and

- The future of the SPCZ is not clear due to model biases in the current climate, and likewise the future behaviour of the ENSO is unclear (see Box in Chapter 1).

There is *low confidence* in the model average rainfall change shown in Table 9.6 because:

- There is a spread in model rainfall projections, which range from a projected rainfall increase to a rainfall decrease;

- The complex set of processes involved in tropical rainfall is challenging to simulate in models. This means that the confidence in the projection of rainfall is generally lower than for other variables such as temperature;

- There is a different magnitude of change in SPCZ rainfall projected by models that have reduced sea-surface temperature biases (Australian Bureau of Meteorology and CSIRO, 2011, Chapter 7 (downscaling); Widlanksy et al., 2012) compared to the CMIP5 models; and

- The future behaviour of the ENSO is unclear, and the ENSO strongly influences year-to-year rainfall variability.

9.5.3 Extremes

Extreme Temperature

The temperature on extremely hot days is projected to increase by about the same amount as average temperature. This conclusion is based on analysis of daily temperature data from a subset of CMIP5 models (Chapter 1). The frequency of extremely hot days is also expected to increase.

The temperature of the 1-in-20-year hot day is projected to increase by approximately 0.5°C by 2030 under the RCP2.6 (very low) scenario and by 0.7°C under the RCP8.5 (very high) scenario. By 2090 the projected increase is 0.7°C for RCP2.6 (very low) and 2.8°C for RCP8.5 (very high).

There is *very high confidence* that the temperature of extremely hot days and the temperature of extremely cool days will increase, because:

- A change in the range of temperatures, including the extremes, is physically consistent with rising greenhouse gas concentrations;

- This is consistent with observed changes in extreme temperatures around the world over recent decades; and

- All the CMIP5 models agree on an increase in the frequency and intensity of extremely hot days and a decrease in the frequency and intensity of cool days.

There is *low confidence* in the magnitude of projected change in extreme temperature because models generally underestimate the current intensity and frequency of extreme events. Changes to the particular driver of extreme temperatures affect whether the change to extremes is more or less than the change in the average temperature, and the changes to the drivers of extreme temperatures in Niue are currently unclear. Also, while all models project the same direction of change there is a wide range in the projected magnitude of change among the models.

Extreme Rainfall

The frequency and intensity of extreme rainfall events are projected to increase. This conclusion is based on analysis of daily rainfall data from a subset of CMIP5 models using a similar method to that in Australian Bureau of Meteorology and CSIRO (2011) with some improvements (Chapter 1), so the results are slightly different to those in Australian Bureau of Meteorology and CSIRO (2011). The current 1-in-20-year daily rainfall amount is projected to increase by approximately 12 mm by 2030 for RCP2.6 and by 13 mm by 2030 for RCP8.5 (very high emissions). By 2090, it is projected to increase by approximately 7 mm for RCP2.6 and by 39 mm for RCP8.5 (very high emissions).The majority of models project the current 1-in-20-year daily rainfall event will become, on average, a 1-in-9-year event for RCP2.6 and a 1-in-4-year event for RCP8.5 (very high emissions) by 2090. These results are different to those found in Australian Bureau of Meteorology and CSIRO (2011) because of different methods used (Chapter 1).

There is *high confidence* that the frequency and intensity of extreme rainfall events will increase because:

- A warmer atmosphere can hold more moisture, so there is greater potential for extreme rainfall (IPCC, 2012);

- Increases in extreme rainfall in the Pacific are projected in all available climate models; and

- An increase in extreme rainfall events within the SPCZ region was found by an in-depth study of extreme rainfall events in the SPCZ (Cai et al., 2012).

There is *low confidence* in the magnitude of projected change in extreme rainfall because:

- Models generally underestimate the current intensity of local extreme events, especially in this area due to the 'cold-tongue bias' (Chapter 1);

- Changes in extreme rainfall projected by models may be underestimated because models seem to underestimate the observed increase in heavy rainfall with warming (Min et al., 2011);

- GCMs have a coarse spatial resolution, so they do not adequately capture some of the processes involved in extreme rainfall events; and

- The Conformal Cubic Atmospheric Model (CCAM) downscaling model has finer spatial resolution and the CCAM results presented in Australian Bureau of Meteorology and CSIRO (2011) indicates a smaller increase in the number of extreme rainfall days, and there is no clear reason to accept one set of models over another.
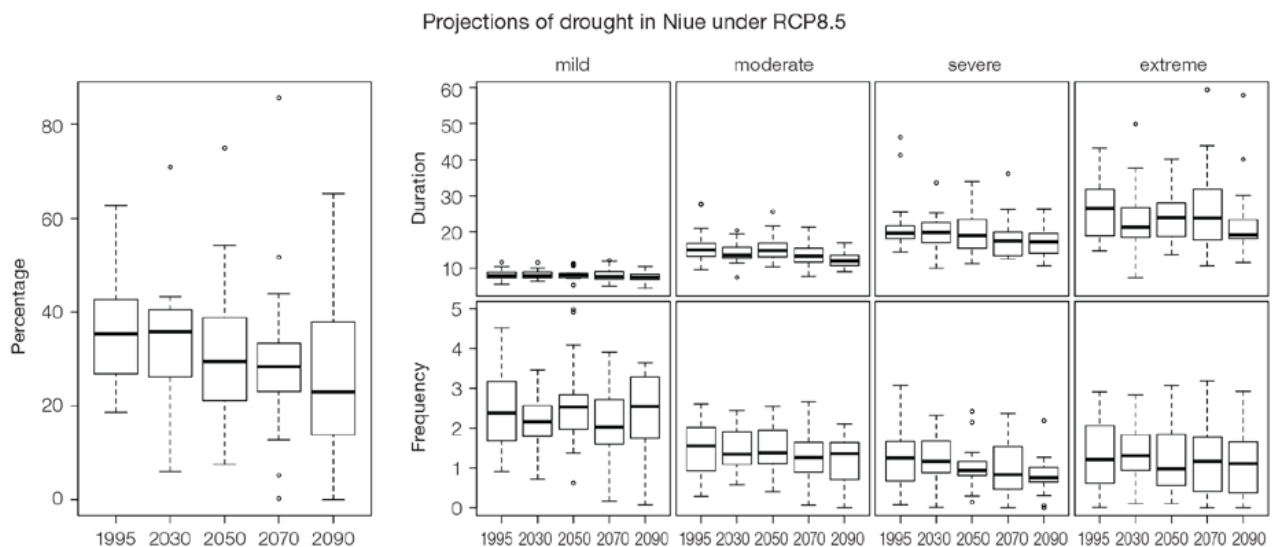
Drought

Drought projections (defined in Chapter 1) are described in terms of changes in proportion of time in drought, frequency and duration by 2090 for very low and very high emissions (RCP2.6 and 8.5).

For Niue the overall proportion of time spent in drought is expected to decrease under RCP8.5 and stay approximately the same under other scenarios (Figure 9.8). Under RCP8.5 the frequency of moderate and severe drought is projected to decrease while the frequencuy of drought in other categories is projected to remain stable. The duration of events in all drought categories is projected to decrease slightly under RCP8.5. Under RCP2.6 (very low emissions) the frequency and duration of drought in all cateogires is projected to remain stable. These results are different from those found in Australian Bureau of Meteorology and CSIRO (2011), which reported a projection of little change in all scenarios.

There is *low confidence* in this direction of change because:

- There is only *low confidence* in the direction of mean rainfall change;

- These drought projections are based upon a subset of models; and

- Like the CMIP3 models, the majority of the CMIP5 models agree on this direction of change.

There is *low confidence* in the projections of drought duration and frequency because there is *low confidence* in the magnitude of rainfall projections, and no consensus about projected changes in the ENSO, which directly influence the projection of drought.

Figure 9.8: Box-plots showing percent of time in moderate, severe or extreme drought (left hand side), and average drought duration and frequency for the different categories of drought (mild, moderate, severe and extreme) for Niue. These are shown for 20-year periods centred on 1995, 2030, 2050, 2070 and 2090 for the RCP8.5 (very high emissions) scenario. The thick dark lines show the median of all models, the box shows the interquartile (25–75%) range, the dashed lines show 1.5 times the interquartile range and circles show outlier results.

Tropical Cyclones

Global Picture

There is a growing level of consistency between models that on a global basis the frequency of tropical cyclones is likely to decrease by the end of the 21st century. The magnitude of the decrease varies from 6%–35% depending on the modelling study. There is also a general agreement between models that there will be an increase in the mean maximum wind speed of cyclones by between 2% and 11% globally, and an increase in rainfall rates of the order of 20% within 100 km of the cyclone centre (Knutson et al., 2010). Thus, the scientific community has a *medium* level of confidence in these global projections.

Niue

In Niue, the projection is for a decrease in cyclone genesis (formation) frequency for the south-east basin (see Figure 9.9 and Table 9.4). The confidence level for this projection is high. The GCMs show consistent results across models for changes in cyclone frequency for the south-east basin, using the direct detection methodologies (OWZ or CDD) described in Chapter 1. Approximately 80% of the projected changes, based on these methods, vary between a 5% decrease to a 50% decrease in genesis frequency with half projecting a decrease between 20 and 40%. The empirical techniques assess changes in the main atmospheric ingredients known to be necessary for cyclone formation. Projections based upon these techniques suggest the conditions for cyclone formation will become less favourable in this region with about half of projected changes indicating decreases between 10 and 40% in genesis frequency. These projections are consistent with those of Australian Bureau of Meteorology and CSIRO (2011).

Table 9.4: Projected percentage change in cyclone frequency in the south-east basin (0–40°S; 170°E–130°W) for 22 CMIP5 climate models, based on five methods, for 2080–2099 relative to 1980–1999 for RCP8.5 (very high emissions). The 22 CMIP5 climate models were selected based upon the availability of data or on their ability to reproduce a current-climate tropical cyclone climatology (See Section 1.5.3 – Detailed Projection Methods, Tropical Cyclones). Blue numbers indicate projected decreases in tropical cyclone frequency, red numbers an increase. MMM is the multi-model mean change. N increase is the proportion of models (for the individual projection method) projecting an increase in cyclone formation.

| Model	GPI change	GPI-M change	Tippett	CDD	OWZ
access10	5	-22	-54	-23	
access13	-26	-26	-36	-10	
bcccsm11	-3	-1	-28		-5
canesm2	-7	-13	-49	-6	
ccsm4				-78	-5
cnrm_cm5	-4	-5	-26	8	7
csiro_mk36	-16	-13	-33	-26	-27
fgoals_g2	6	-8	-40		
fgoals_s2	-15	-20	-48		
gfdl_esm2m				-48	-36
gfdl_cm3	-1	-5	-25		-11
gfdl_esm2g				-18	-36
gisse2r	17	16	-6		
hadgem2_es	-8	-11	-51		
inm	-3	-3	-30		
ipslcm5alr	-13	-19	-43		
ipslcm5blr				7	
miroc5				-43	-22
mirocesm	-40	-38	46		
mpim	-26	-19	-41		
mricgcm3	-8	-10	-28		
noresm1m	-36	-40	-59	-80	
MMM	-11	-14	-32	-29	-17
N increase	0.2	0.1	0.1	0.2	0.125
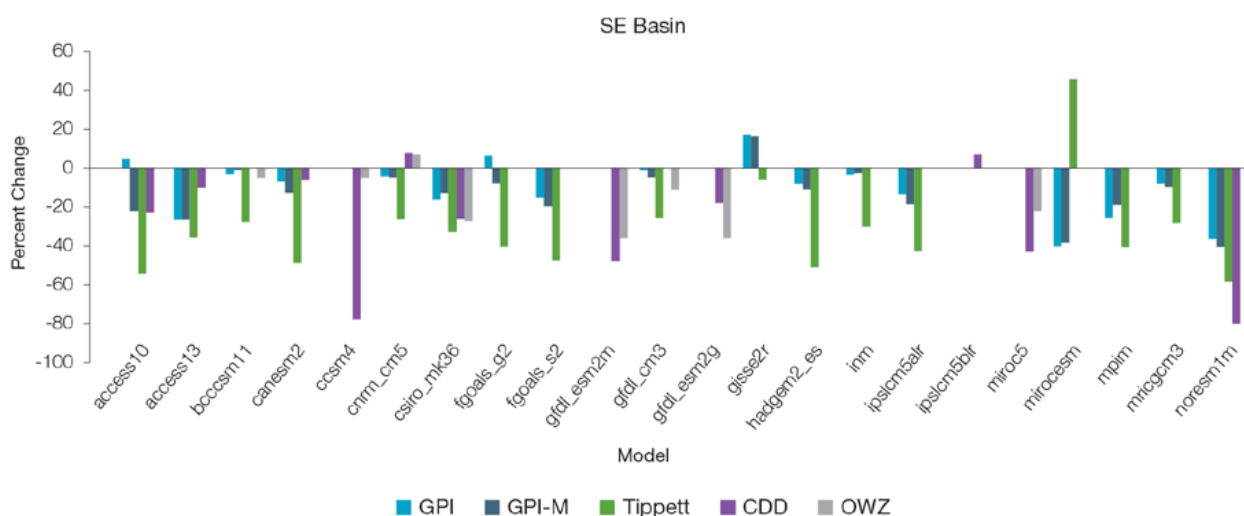
Figure 9.9: Projected percentage change in cyclone frequency in the south-east basin (data from Table 9.4).

9.5.4 Coral Reefs and Ocean Acidification

As atmospheric CO_2 concentrations continue to rise, oceans will warm and continue to acidify. These changes will impact the health and viability of marine ecosystems, including coral reefs that provide many key ecosystem services (*high confidence*). These impacts are also likely to be compounded by other stressors such as storm damage, fishing pressure and other human impacts.

The projections for future ocean acidification and coral bleaching use three RCPs (2.6, 4.5, and 8.5).

Ocean Acidification

Ocean acidification is expressed in terms of aragonite saturation state (Chapter 1). In Niue the aragonite saturation state has declined from about 4.5 in the late 18th century to an observed value of about 4.0±0.1 by 2000 (Kuchinke et al., 2014). All models show that the aragonite saturation state, a proxy for coral reef growth rate, will continue to decrease as atmospheric CO_2 concentrations increase (*very high confidence*). Projections from CMIP5 models indicate that under RCPs 8.5 (very high emissions) and 4.5 (low emissions) the median aragonite saturation state will transition to marginal conditions (3.5) around 2030. In RCP8.5 (very high emissions) the aragonite saturation state continues to strongly decline thereafter to

values where coral reefs have not historically been found (< 3.0). Under RCP4.5 (low emissions) the aragonite saturation plateaus around 3.2 i.e. marginal conditions for healthy coral reefs. While under RCP2.6 (very low emissions) the median aragonite saturation state never falls below 3.5, and increases slightly toward the end of the century (Figure 9.10) suggesting that the conditions remains adequate for healthy corals reefs. There is *medium confidence* in this range and distribution of possible futures because the projections are based on climate models that do not resolve the reef scale that can play a role in modulating large-scale changes. The impacts of ocean acidification are also likely to affect the entire marine ecosystem impacting the key ecosystem services provided by reefs.
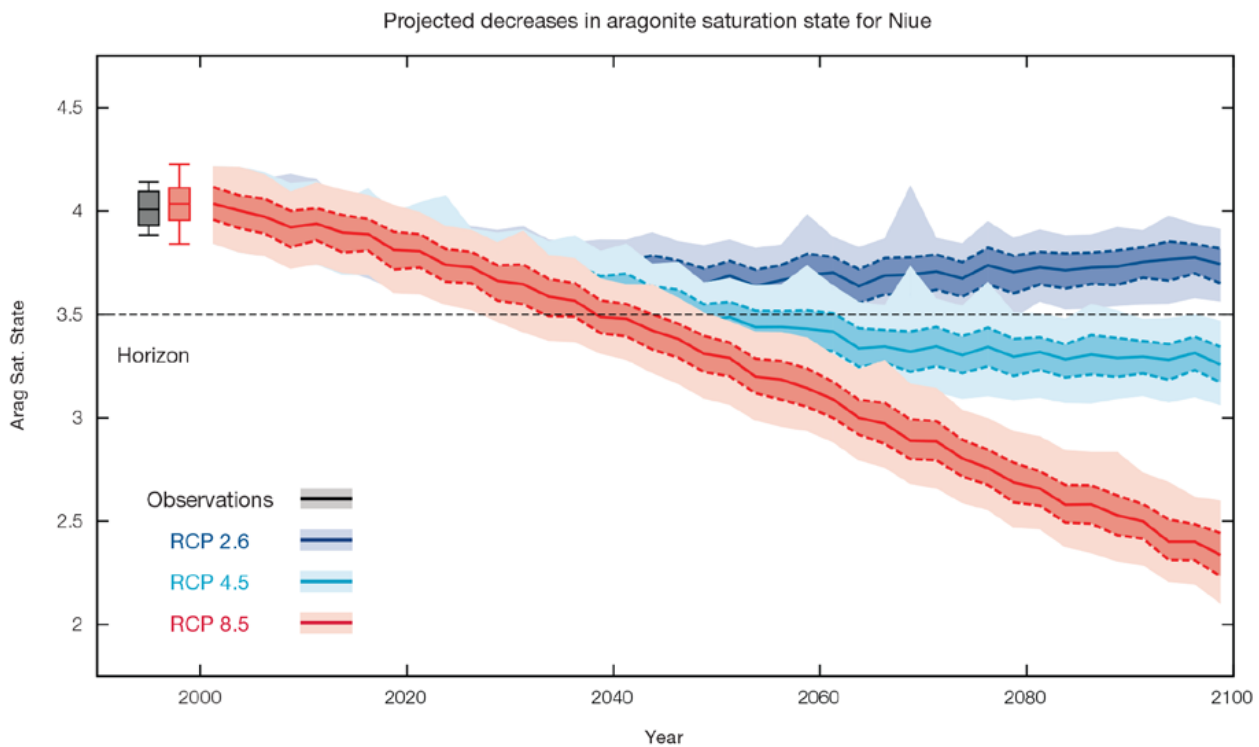
Figure 9.10: Projected decreases in aragonite saturation state in Niue from CMIP5 models under RCP2.6, 4.5 and 8.5. Shown are the median values (solid lines), the interquartile range (dashed lines), and 5% and 95% percentiles (light shading). The horizontal line represents the transition to marginal conditions for coral reef health (from Guinotte et al., 2003).

Coral Bleaching Risk

As the ocean warms, the risk of coral bleaching increases (*very high confidence*). There is *medium confidence* in the projected rate of change for Niue because there is *medium confidence* in the rate of change of sea-surface temperature (SST), and the changes at the reef scale (which can play a role in modulating large-scale changes) are not adequately resolved. Importantly, the coral bleaching risk calculation does not account the impact of other potential stressors (Chapter 1).

The changes in the frequency (or recurrence) and duration of severe bleaching risk are quantified for different projected SST changes (Table 9.5). Overall there is a decrease in the time between two periods of

elevated risk and an increase in the duration of the elevated risk. For example, under a long-term mean increase of 1°C (relative to 1982–1999 period), the average period of severe bleaching risk (referred to as a risk event will last 8.1 weeks (with a minimum duration of 2.9 weeks and a maximum duration of 3.0 months) and the average time between two risks will be 3.0 years (with the minimum recurrence of 10.3 months and a maximum recurrence of 6.7 years). If severe bleaching events occur more often than once every five years, the long-term viability of coral reef ecosystems becomes threatened.

9.5.5 Sea Level

Mean sea level is projected to continue to rise over the course of the 21st century. There is very *high confidence* in the direction of change. The CMIP5 models simulate a rise of between approximately 7–18 cm by 2030 (very similar values for different RCPs), with increases of 41–87 cm by 2090 under the RCP8.5 (Figure 9.11 and Table 9.6). There is *medium confidence* in the range mainly because there is still uncertainty associated with projections of the Antarctic ice sheet contribution. Interannual variability of sea level will lead to periods of lower and higher regional sea levels. In the past, this interannual variability has been about 17 cm (5–95% range, after removal of the seasonal signal, see dashed lines in Figure 9.11 (a) and it is likely that a similar range will continue through the 21st century.

Table 9.5: Projected changes in severe coral bleaching risk for the Niue EEZ for increases in SST relative to 1982–1999.

Temperature change [1]	Recurrence interval [2]	Duration of the risk event [3]
Change in observed mean	0	0
+0.25°C	0	0
+0.5°C	30 years	5.0 weeks
+0.75°C	16.0 years (9.7 years – 23.2 years)	6.9 weeks (5.5 weeks – 8.6 weeks)
+1°C	3.0 years (10.3 months – 6.7 years)	8.1 weeks (2.9 weeks – 3.0 months)
+1.5°C	1.0 years (4.0 months – 2.7 years)	3.0 months (2.4 weeks –5.1 months)
+2°C	8.4 months (6.0 months – 1.5 years)	4.4 months (1.5 months – 6.8 months)

[1] This refers to projected SST anomalies above the mean for 1982–1999.
[2] Recurrence is the mean time between severe coral bleaching risk events. Range (min – max) shown in brackets.
[3] Duration refers to the period of time where coral are exposed to the risk of severe bleaching. Range (min – max) shown in brackets.

Observed and projected relative sea-level change near Niue
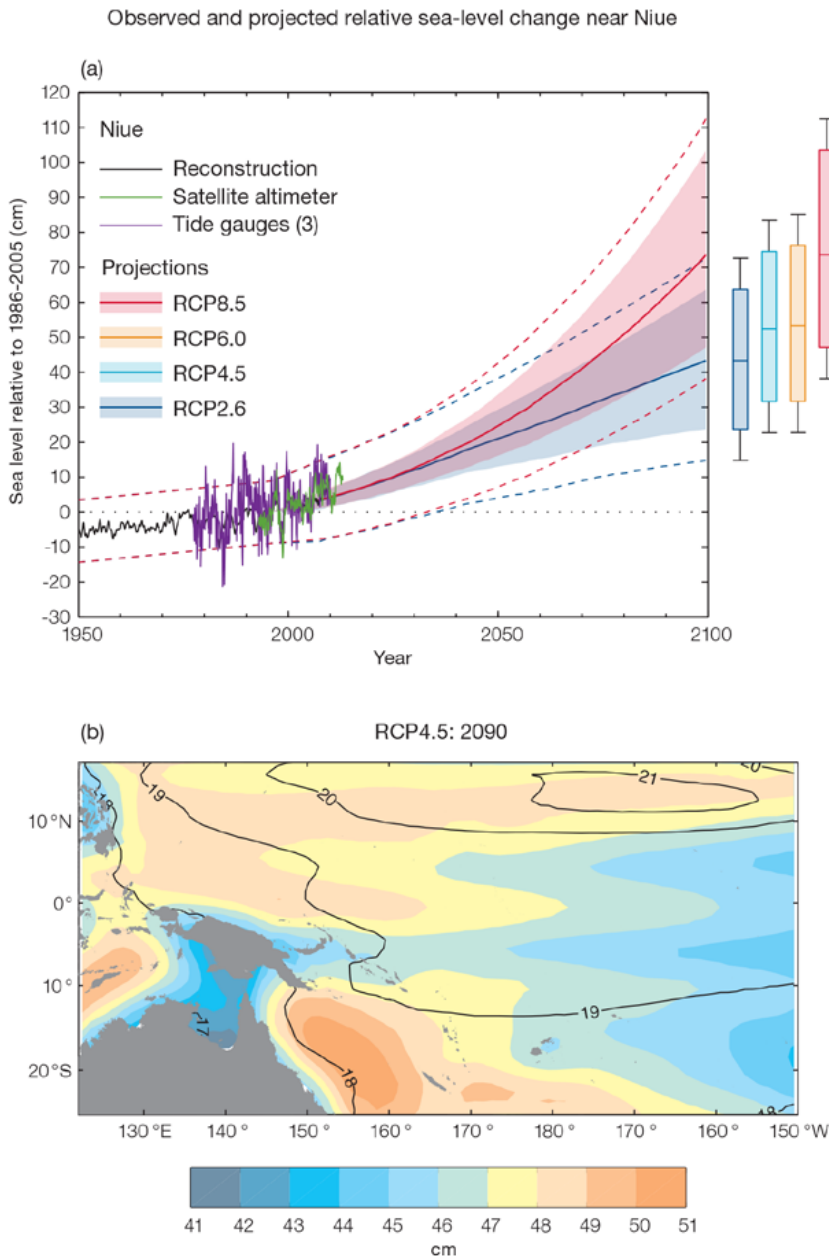
Figure 9.11: (a) The observed tide-gauge records of relative sea-level (since the late 1970s) are indicated in purple, and the satellite record (since 1993) in green. The gridded (reconstructed) sea level data at Niue (since 1950) is shown in black. Multi-model mean projections from 1995–2100 are given for the RCP8.5 (red solid line) and RCP2.6 emissions scenarios (blue solid line), with the 5–95% uncertainty range shown by the red and blue shaded regions. The ranges of projections for four emission scenarios (RCPs 2.6, 4.5, 6.0 and 8.5) by 2100 are also shown by the bars on the right. The dashed lines are an estimate of interannual variability in sea level (5–95% uncertainty range about the projections) and indicate that individual monthly averages of sea level can be above or below longer-term averages.

(b) The regional distribution of projected sea level rise under the RCP4.5 emissions scenario for 2081–2100 relative to 1986–2005. Mean projected changes are indicated by the shading, and the estimated uncertainty in the projections is indicated by the contours (in cm).

9.5.6 Wind-driven Waves

During December–March at Niue, projected changes in wave properties include a decrease in wave height (Figure 9.12), accompanied by a slight decrease in wave period and no significant rotation *(low confidence)* (Table 9.7). These features are characteristic of a decrease in strength of the south-easterly trade winds. This change is only statistically significant by the end of the century in a high emission scenario and only in December, January and March, with a projected decrease in wave height of approximately 8 cm.

In June–September, projected changes include a small anticlockwise rotation toward the east, with no change in wave height or period *(low confidence)* (Table 9.7). No change is projected in larger waves *(low confidence)*.

There is *low confidence* in projected changes in the Niue wind-wave climate because:

- Projected changes in wave climate are dependent on confidence in projected changes in the ENSO, which is low; and

- The differences between simulated and observed (hindcast) wave data can be larger than the projected wave changes, which further reduces our confidence in projections.
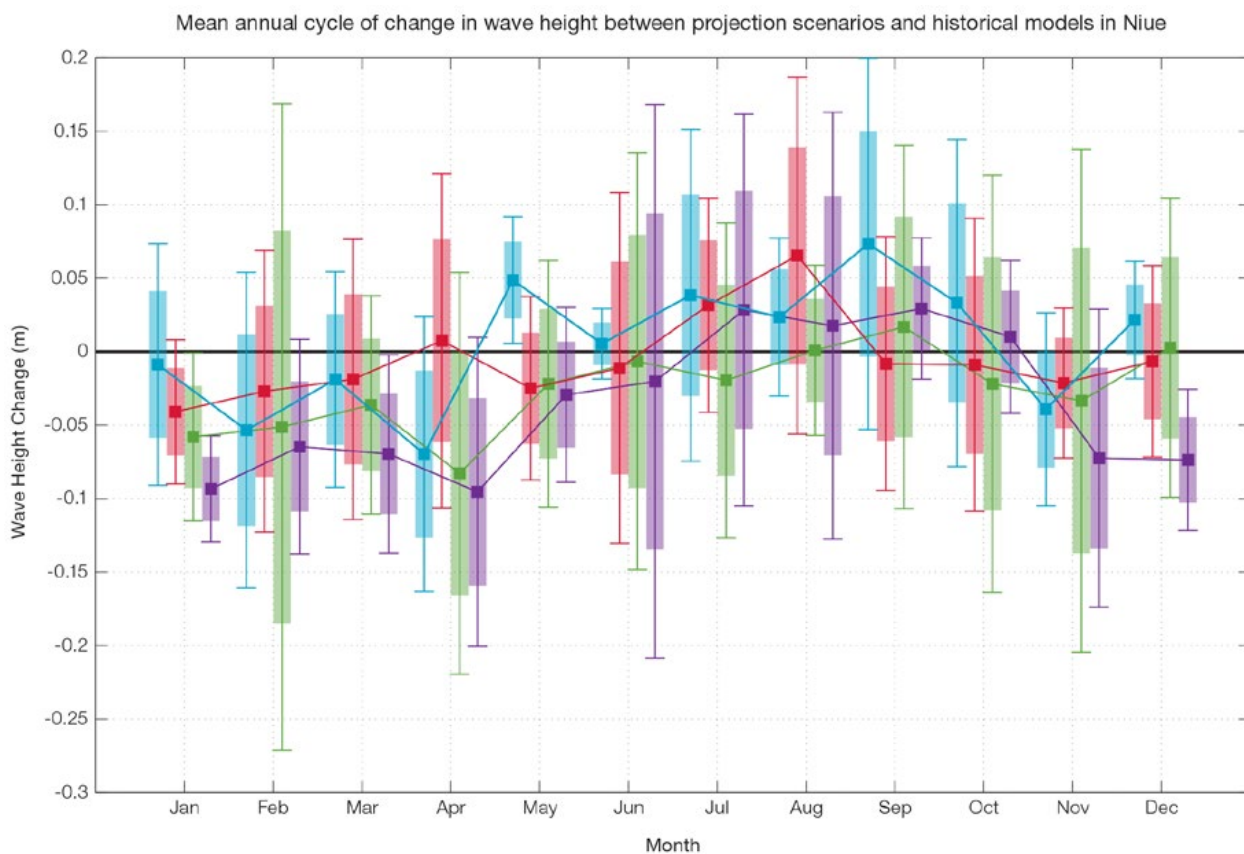
Figure 9.12: Mean annual cycle of change in wave height between projection scenarios and historical models in Niue. This plot shows a non-significant decrease in wave heights in the wet season months (apart from RCP8.5, very high emissions, December, January and March 2090 which are significant), and no change in the dry season months. Shaded boxes show 1 standard deviation of models' means around the ensemble means, and error bars show the 5–95% range inferred from the standard deviation. Colours represent RCP scenarios and time periods: blue 2035 RCP4.5 (low emissions), red 2035 RCP8.5 (very high emissions), green 2090 RCP4.5 (low emissions), purple 2090 RCP8.5 (very high emissions).

9.5.7 Projections Summary

There is *very high confidence* in the direction of long-term change in a number of key climate variables, namely an increase in mean and extremely high temperatures, sea level and ocean acidification. There is *high confidence* that the frequency and intensity of extreme rainfall will increase. There is *low confidence* that annual rainfall will increase slightly and drought incidence will decrease slightly.

Tables 9.6 and 9.7 quantify the mean changes and ranges of uncertainty for a number of variables, years and emissions scenarios. A number of factors are considered in assessing confidence, i.e. the type, amount, quality and consistency of evidence (e.g. mechanistic understanding, theory, data, models, expert judgment) and the degree of agreement, following the IPCC guidelines (Mastrandrea et al., 2010). Confidence ratings in the projected magnitude of mean change are generally lower than those for the direction of change (see paragraph above) because magnitude of change is more difficult to assess. For example, there is *very high confidence* that temperature will increase, but *medium confidence* in the magnitude of mean change.

Table 9.6: Projected changes in the annual and seasonal mean climate for Niue under four emissions scenarios; RCP2.6 (very low emissions, in dark blue), RCP4.5 (low emissions, in light blue), RCP6 (medium emissions, in orange) and RCP8.5 (very high emissions, in red). Projected changes are given for four 20-year periods centred on 2030, 2050, 2070 and 2090, relative to a 20-year period centred on 1995. Values represent the multi-model mean change, with the 5–95% range of uncertainty in brackets. Confidence in the magnitude of change is expressed as *high*, *medium* or *low*. Surface air temperatures in the Pacific are closely related to sea-surface temperatures (SST), so the projected changes to air temperature given in this table can be used as a guide to the expected changes to SST. (See also Section 1.5.2). 'NA' indicates where data are not available.

Variable	Season	2030	2050	2070	2090	Confidence (magnitude of change)
Surface air temperature (°C)	Annual	0.5 (0.3 to 0.9)	0.6 (0.3 to 1)	0.6 (0.3 to 1)	0.6 (0.2 to 1.1)	*Medium*
		0.5 (0.3 to 0.9)	0.8 (0.6 to 1.5)	1.1 (0.7 to 1.8)	1.2 (0.7 to 2.1)	
		0.5 (0.3 to 0.9)	0.8 (0.5 to 1.4)	1.2 (0.8 to 1.9)	1.6 (1.1 to 2.5)	
		0.6 (0.4 to 1.1)	1.2 (0.8 to 2)	1.9 (1.3 to 3)	2.6 (1.7 to 4.2)	
Maximum temperature (°C)	1-in-20 year event	0.5 (0.2 to 0.8)	0.6 (0.2 to 0.9)	0.7 (0.1 to 1.1)	0.7 (0.1 to 1.2)	*Medium*
		0.5 (0.2 to 1)	0.9 (0.5 to 1.3)	1.1 (0.6 to 1.5)	1.2 (0.6 to 1.8)	
		NA (NA to NA)	NA (NA to NA)	NA (NA to NA)	NA (NA to NA)	
		0.7 (0.2 to 1.3)	1.4 (0.7 to 1.9)	2.1 (1.3 to 2.9)	2.8 (1.9 to 3.9)	
Minimum temperature (°C)	1-in-20 year event	0.5 (-0.1 to 0.9)	0.6 (0.1 to 1)	0.7 (0.4 to 1)	0.7 (-0.1 to 1.1)	*Medium*
		0.5 (-0.2 to 0.9)	0.9 (0.3 to 1.4)	1.2 (0.6 to 1.8)	1.2 (0.6 to 1.9)	
		NA (NA to NA)	NA (NA to NA)	NA (NA to NA)	NA (NA to NA)	
		0.8 (0.3 to 1.2)	1.4 (0.7 to 2.2)	2.1 (1.4 to 3)	2.9 (2.1 to 4.6)	
Total rainfall (%)	Annual	2 (-9 to 11)	1 (-13 to 12)	1 (-8 to 12)	1 (-12 to 11)	*Low*
		0 (-11 to 12)	0 (-17 to 16)	3 (-18 to 16)	2 (-12 to 22)	
		1 (-10 to 12)	3 (-6 to 15)	6 (-9 to 27)	6 (-12 to 27)	
		1 (-12 to 18)	1 (-14 to 13)	4 (-16 to 32)	7 (-12 to 46)	
Total rainfall (%)	Nov-Apr	3 (-13 to 15)	2 (-13 to 18)	1 (-10 to 11)	0 (-17 to 12)	*Low*
		1 (-13 to 16)	1 (-18 to 21)	4 (-16 to 24)	3 (-14 to 31)	
		3 (-10 to 19)	3 (-10 to 16)	6 (-11 to 33)	7 (-14 to 33)	
		1 (-18 to 21)	2 (-16 to 17)	6 (-19 to 45)	10 (-14 to 67)	
Total rainfall (%)	May-Oct	1 (-8 to 9)	1 (-11 to 13)	1 (-9 to 11)	2 (-5 to 11)	*Low*
		0 (-9 to 12)	0 (-15 to 12)	3 (-16 to 19)	2 (-13 to 14)	
		-2 (-13 to 7)	4 (-5 to 14)	5 (-6 to 16)	5 (-6 to 25)	
		1 (-11 to 13)	1 (-11 to 13)	1 (-15 to 16)	4 (-15 to 31)	
Aragonite saturation state (Ωar)	Annual	-0.3 (-0.6 to 0.0)	-0.4 (-0.7 to -0.1)	-0.4 (-0.7 to -0.1)	-0.3 (-0.7 to 0.0)	*Medium*
		-0.4 (-0.6 to -0.1)	-0.6 (-0.8 to -0.3)	-0.7 (-1.0 to -0.4)	-0.8 (-1.0 to -0.5)	
		NA (NA to NA)	NA (NA to NA)	NA (NA to NA)	NA (NA to NA)	
		-0.4 (-0.7 to -0.1)	-0.7 (-1.0 to -0.5)	-1.1 (-1.4 to -0.9)	-1.5 (-1.8 to -1.3)	
Mean sea level (cm)	Annual	12 (7 to 17)	21 (13 to 30)	30 (18 to 43)	40 (23 to 57)	*Medium*
		12 (8 to 17)	22 (14 to 31)	34 (22 to 47)	47 (29 to 66)	
		12 (7 to 17)	22 (13 to 30)	34 (21 to 47)	47 (29 to 67)	
		13 (8 to 18)	25 (16 to 34)	42 (27 to 57)	62 (41 to 87)	

Waves Projections Summary

Table 9.7: Projected average changes in wave height, period and direction at Niue for December–March and June–September for RCP4.5 (low emissions, in blue) and RCP8.5 (very high emissions, in red), for two 20-year periods (2026–2045 and 2081–2100), relative to a 1986–2005 historical period. The values in brackets represent the 5th to 95th percentile range of uncertainty.

Variable	Season	2035	2090	Confidence (range)
Wave height change (m)	December–March	0.0 (-0.2 to 0.2) -0.0 (-0.2 to 0.2)	-0.0 (-0.3 to 0.2) -0.1 (-0.3 to 0.1)	Low
	June–September	+0.0 (-0.3 to 0.4) +0.0 (-0.3 to 0.4)	0.0 (-0.4 to 0.4) 0.0 (-0.4 to 0.4)	Low
Wave period change (s)	December–March	-0.1 (-1.1 to 1.0) -0.1 (-1.1 to 0.9)	-0.1 (-1.2 to 1.1) -0.2 (-1.4 to 1.2)	Low
	June–September	0.0 (-0.9 to 0.9) 0.0 (-0.9 to 0.9)	0.0 (-1.0 to 1.0) -0.0 (-1.1 to 1.1)	Low
Wave direction change (° clockwise)	December–March	0 (-30 to 30) 0 (-30 to 30)	-0 (-30 to 30) -0 (-40 to 30)	Low
	June–September	-0 (-10 to 10) -0 (-10 to 10)	-0 (-10 to 10) -5 (-10 to 5)	Low

Wind-wave variables parameters are calculated for a 20-year period centred on 2035.